Research Article

Vibration Analysis of Tubular Profiled Shafts

P. M. G. Bashir Asdaque[Á*], R. K. Behera[Á]

[Á]Department of Mechanical Engineering, N.I.T. Rourkela, Rourkela, India

Abstract

Shaft-rotor systems consisting of tubular profiled shafts with uniform thickness are taken into consideration. The computation of deflection, slope, shear force and bending moment at the extremities of the tubular-shaft are done using conventional mathematical procedures. Whirling frequency conditions are computed using transfer matrix method. The response of the system for different profiles, lengths and speeds are computed and plotted for better understanding. The results are compared with previous published works. The step response of the system is also plotted to show the effects of gyroscopic couples at different speeds. Further, combined FEM and transfer matrix method is demonstrated for analyzing the non-rotating shafts with complex geometries.

Keywords: Profiled, Response, Shaft, Vibration, Whirling.

1. Introduction

Shaft is an important component of the rotating system, mainly used to transmit torque and rotation. Hence the study and stability of shaft-rotor systems has been the concern of researchers for more than a century, and will continue to persist as an active area of research and analysis in coming future. Shaft geometry is of the main concern during the study of any rotating machines. Most of the papers related to rotating machines consider cylindrical shaft elements for the study and analysis of rotating systems, as in (Nelson and McVaugh, 1976). The first idea of transfer matrix method (TMM) was put forth by Holzer for finding natural frequencies of torsional systems and later adapted by Myklestad for calculating natural frequencies of airplane wing, coupled in bending and torsion (Myklestad, 1944), (Myklestad, 1945). Prohl applied it to rotor-bearing systems and included gyroscopic moments in his computations (Prohl, 1945). Lund used complex variables as the next significant advancement in the method (Lund, 1974). An improved method for calculating critical speeds and rotor stability of turbo machinery was investigated, as in (Murphy and Vance, 1983). Whalley and Ameer used frequency response analysis for particular profiled shafts to study dynamic response of distributed-lumped shaft rotor system. They studied the system behavior in terms of frequency response for the shafts with diameters which are functions of their lengths. They derived an analytical method which uses Euler-Bernoulli beam theory in combination with TMM (Whalley and Ameer, 2009). On the other hand, there are large number of numerical

applications of finite element techniques for the calculation of whirling and the computation of maximum dynamic magnitude. In this regard, Ruhl and Booker modeled the distributed parameter turbo rotor systems using FEM (Ruhl and Booker, 1972). Nelson and McVaugh reduced large number of eigenvalues and eigenvectors identified, following finite element analysis, and the erroneous modes of vibration predicted were eliminated (Nelson and McVaugh, 1976).

Using the the transfer matrix approach (Whalley and Ameer, 2009), the dynamic analysis of tubular-profiled shaft has been done. The finite element method is avoided for rotor dynamics as it produces matrices of very large order. The impact of length and speed on the dynamic analysis of the tubular-shaft-rotor system is also clearly shown. Frequency response of the rotor-system for an impulse of 1N is determined in terms of critical speed for various profile values, shaft speed and shaft lengths. Step response of the system is also found to demonstrate the effects of gyroscopic couple. Further, combined finite element method and transfer matrix method (Tang and Wu, 2012) is demonstrated for analyzing the non-rotating condition of tubular profiled shafts.

2. Shaft model

Input and output relationship for deflection, slope, bending moment and shear force for the distributed parameter shaft model (Whalley and Ameer, 2009) is given by

$$(y_2, \theta_2, M_{y2}, Q_{y2})^T = F(s)\,(y_1, \theta_1, M_{y1}, Q_{y1})^T$$

Where

---

*Corresponding author: P. M. G. Bashir Asdaque

$$F(s) = \begin{bmatrix} f_1 & \dfrac{f_2}{2\gamma(0)} & \dfrac{-c(0)l^2 f_3}{2\gamma^2(0)} & \dfrac{-c(0)l^3 f_4}{2\gamma^3(0)} \\[2ex] \dfrac{\gamma(0)f_4}{2l} & f_1 & \dfrac{-c(0)lf_2}{2\gamma(0)} & \dfrac{-c(0)l^2 f_3}{2\gamma^2(0)} \\[2ex] \dfrac{-\gamma^2(0)f_3}{2l^2 c(0)} & \dfrac{-\gamma(0)f_4}{2c(0)l} & f_1 & \dfrac{f_2}{2\gamma(0)} \\[2ex] \dfrac{-\gamma^3(0)f_2}{2c(0)l^3} & \dfrac{-\gamma^2(0)f_3}{2l^2 c(0)} & \dfrac{\gamma(0)f_4}{2l} & f_1 \end{bmatrix}$$

Where

$$f_1 = (\cosh \gamma(l) + \cos \gamma(l)) / 2$$
$$f_2 = (\sinh \gamma(l) + \sin \gamma(l)) / 2$$
$$f_3 = (\cosh \gamma(l) - \cos \gamma(l))$$
$$f_4 = (\sinh \gamma(l) - \sin \gamma(l))$$
$$\gamma(x) = l\sqrt{\Gamma(x)}$$
$$\Gamma^{\frac{1}{2}}(x) = s^{\frac{1}{2}}(L(x)c(x))^{\frac{1}{4}}$$
$$c(x) = \frac{1}{EI(x)}$$

The complete derivation of F(s) can be found in (Whalley and Ameer, 2009).

3. Rigid disc

The output vector from the shaft will become the input for the rigid disc model, as shown in Fig. 1. i.e., for disk model, we have,

$$y_3(s) = y_2(s)$$
$$\theta_3(s) = \theta_2(s)$$
$$M_{y3}(s) = M_{y2}(s) - J\Omega s\theta_2(s)$$
$$Q_{y3}(s) = ms^2 y_2(s) + Q_{y2}(s)$$

Hence, writing in matrix form, one have

$$(y_3(s), \theta_3(s), M_{y3}(s), Q_{y3}(s))^T =$$
$$R(s)(y_2(s), \theta_2(s), M_{y2}(s), Q_{y2}(s))$$

Where $R(s) = \begin{bmatrix} 1 & 0 & 0 & 0 \\ 0 & 1 & 0 & 0 \\ 0 & -J\Omega s & 1 & 0 \\ ms^2 & 0 & 0 & 1 \end{bmatrix}$
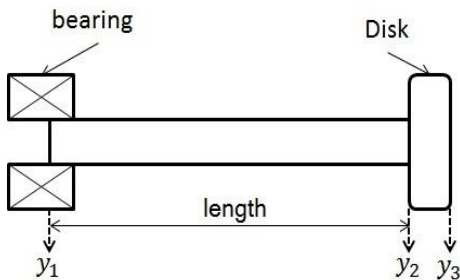

Fig. 1 Shaft with rigid disk

4. Numerical results

4.1 Rotating tubular profiled shaft-rotor system

A cantilever rotor shaft system with a disk at free end is shown for illustration purposes Fig. 1. Effects of bearings are neglected. As we proceeded in above sections, in the same way for the system illustrated in Fig.2 can be formulated as-

$$H(s) = R(s)F(s)$$

Where

$(y_3(s), y_1(s)), (\theta_3(s), \theta_1(s)), (M_{y3}(s), M_{y1}(s))$ and $(Q_{y1}(s), Q_{y1}(s))$

are the deflections, slopes, Bending moments and shear forces at the free and fixed end respectively.

Also,

$$H(s) = \begin{bmatrix} H_{11} & H_{12} \\ H_{21} & H_{22} \end{bmatrix}$$

Input-output vectors relationship is given by:

$$\begin{bmatrix} y_3 \\ \theta_3 \\ M_{y3} \\ Q_{y3} \end{bmatrix} = H(s) \begin{bmatrix} y_1 \\ \theta_1 \\ M_{y1} \\ Q_{y1} \end{bmatrix}$$

After applying the boundary conditions for cantilever beam, we get deflection y_3 at the free end of the system, so we will ultimately get the transfer function, where the profile equation (Whalley and Ameer, 2009) of the shaft-rotor is given by

$$r(x) = r0(1 - NN(x^2))$$

Since the shaft is tubular, let the outer diameter and inner diameters are d_o and d_i respectively.

For example, transfer function for NN=25, l=0.1m, t=0.002 m, E=209x10^9 Pa, m=0.7443 Kg, D=0.09 and rotational speed of 10000 rpm is:

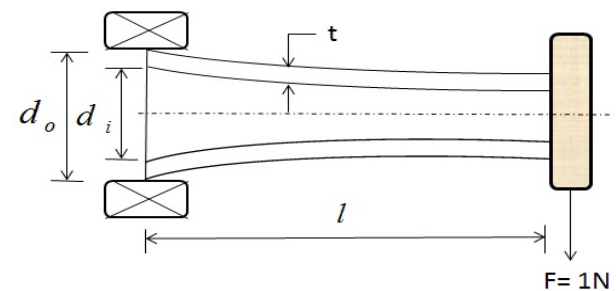$$\frac{1.344\ s + 1.025 \times 10^4}{s^3 + 7626\ s^2 + 8.608 \times 10^5\ s + 1.641 \times 10^9}$$

Fig. 2 Tubular profiled shaft with uniform thickness t and force of 1 N on the disc

Table 1 Default values for the system illustrated in Fig. 2

Parameters	Values
Length of the shaft-rotor, l (m)	0.1
Mass of the disk, m (Kg)	0.7443
Diameter of the disk, D (m)	0.09
Young's Modulus of Elasticity, E (GPa)	209
Density of the material, ρ (Kg/m^3)	7800
Rotational Speed, N (rpm)	10000
Thickness of the tubular shaft, t (m)	0.002
Profile Value, NN (Constant)	25

4.1.1 Varying profile value (NN)

Bode plot has been obtained for different profiles of the shaft-rotor system by changing the profile values of NN in (5) of the shaft, as shown in Fig. 3. Critical frequencies obtained for tubular profiled shafts are tabulated and compared with that of solid profiled shafts (Whalley and Ameer, 2009) in Table 2.
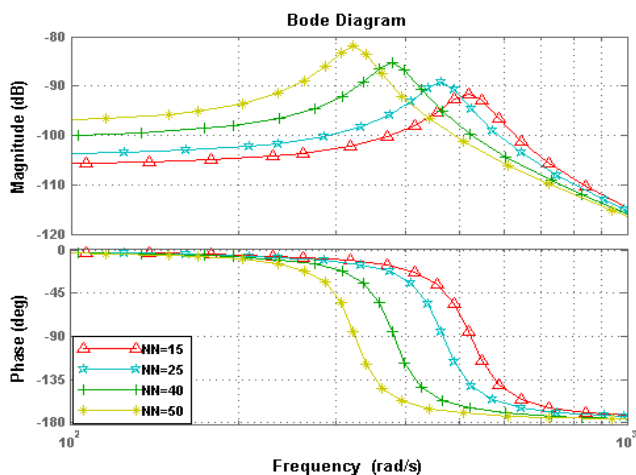

Fig. 3. Bode plot for different NN values

Table 2 Critical frequencies for Tubular and Solid profiled shafts

Value of NN	Critical Frequency (Tubular Shaft) (rad/s)	Critical Frequency (Solid Shaft) (rad/s)
15	518	583.043
25	463	531.550
40	378	456.430
50	322	394.290

4.1.2. Effect of different shaft length

The study of changing length is considered to be of great use dealing with the resonance conditions. Bode plot has been obtained for different lengths of the shaft-rotor segments as shown in Fig. 4.
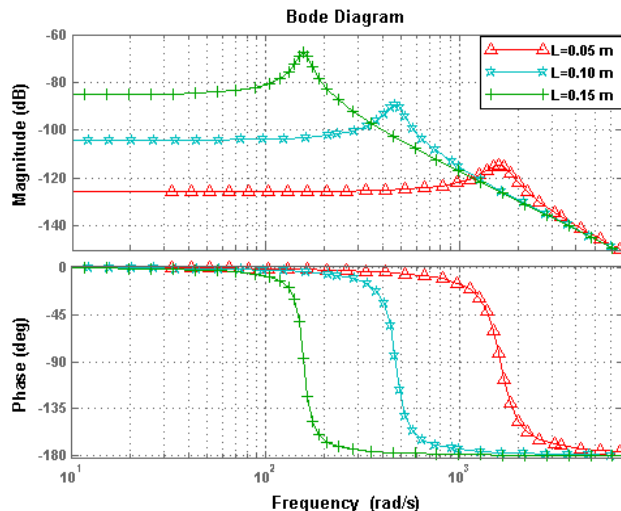

Fig. 4. Bode plot for different shaft lengths

4.1.3. Changing rotor speed

The Bode plot has been obtained for changing rotor speeds for 2000, 4000, 6000 and 10000 rpm as shown in Fig. 5. It may be noticed that the effect of rotational speeds on the critical frequency is negligible, however the impact on amplitude can be felt via bode plot.
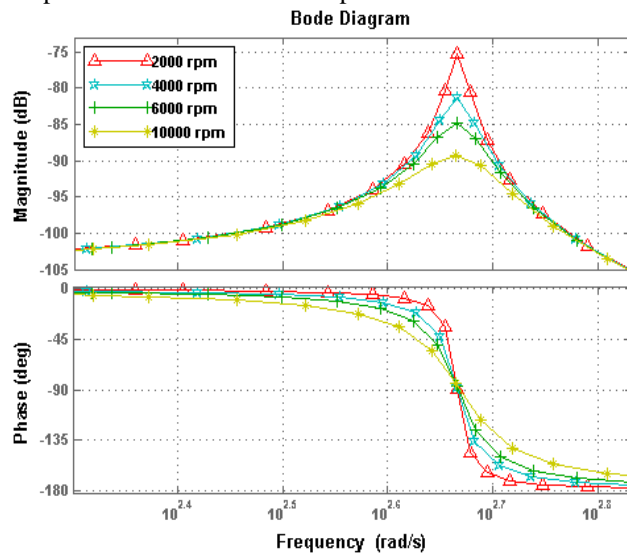

Fig. 5. Bode plot for different rotational speeds

4.1.4. Step Response

For NN=25, at 10000 rpm, the step response, following an impulse of 1 N, gives the characteristics shown in Fig 6. It shows the steady state conditions will be restored in approximately 0.0891 s. At lesser rotational speeds the effects of this disturbance would be greater because of the reduction in the gyroscopic couple. In Fig.6, at 5000 rpm the maximum overshoot remains unchanged, but settling time is almost double than for 10000 rpm, i.e., 0.183 s, after the same impulse disturbance, and hence is the effect of gyroscopic couple. As shown herein, this reveals a part of the problem.
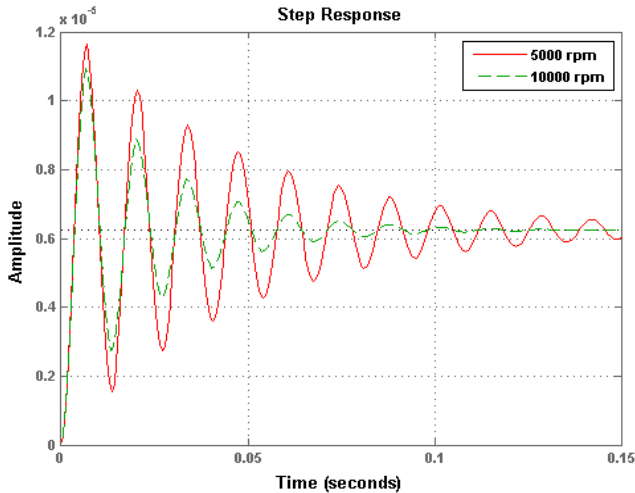
Fig. 6. Step response for two different speeds

4.2.Non-rotating tubular profiled shaft

Combined FEM and TMM for tip deflection of a tubular profiled cantilever beam in pure bending has been demonstrated in this section using the approach of combined TMM and FEM (Tang and Wu, 2012). This part is shown here for easy combination of FEM and TMM is computing deflections of complex geometries. The equation for the stiffness matrix from energy method is given by

$$K = \int_0^l EI(x)(\frac{\partial^2 N}{\partial x^2})^T (\frac{\partial^2 N}{\partial x^2})dx$$

Where E is the young's modulus and $I(x)$ is the inertia for the tubular shaft which is the function of its length.

$$I(x) = \frac{\pi(d_o^4(x) - d_i^4(x))}{64}$$

N is the shape function for Euler-Bernoulli beam (Reddy, 1984).

$$N = \begin{bmatrix} N_1 & N_2 & N_3 & N_4 \end{bmatrix}$$

Where

$$N_1 = 1 - 3\frac{x^2}{l^2} + 2\frac{x^3}{l^3}$$

$$N_2 = x - 2\frac{x^2}{l} + \frac{x^3}{l^2}$$

$$N_3 = 3\frac{x^2}{l^2} - 2\frac{x^3}{l^3}$$

$$N_4 = -\frac{x^2}{l} + \frac{x^3}{l^2}$$

The K matrix obtained after integration is very large, so for easy understanding, stiffness matrix for the tubular shaft shown in Fig. 7 be represented by:

$$K = \begin{bmatrix} K_{11} & K_{12} & K_{13} & K_{14} \\ K_{21} & K_{22} & K_{23} & K_{24} \\ K_{31} & K_{32} & K_{33} & K_{34} \\ K_{41} & K_{42} & K_{43} & K_{44} \end{bmatrix}$$

Assume the force and torque on the nodes of fixed and free end, as shown in Fig. are F_1, M_1, F_2 and M_2 divide the 4-order stiffness matrix K obtained into four 2-order matrices T_{11}, T_{12}, T_{21} and T_{22} respectively:

$$\begin{Bmatrix} F_1 \\ M_1 \\ F_2 \\ M_2 \end{Bmatrix} = \begin{bmatrix} T_{11} & T_{12} \\ T_{21} & T_{22} \end{bmatrix} \begin{Bmatrix} y_1 \\ \theta_1 \\ y_2 \\ \theta_2 \end{Bmatrix}$$

Where

$$T_{11} = \begin{bmatrix} K_{11} & K_{12} \\ K_{21} & K_{22} \end{bmatrix}, T_{12} = \begin{bmatrix} K_{13} & K_{14} \\ K_{23} & K_{24} \end{bmatrix}$$

$$T_{21} = \begin{bmatrix} K_{31} & K_{32} \\ K_{41} & K_{42} \end{bmatrix}, T_{22} = \begin{bmatrix} K_{33} & K_{34} \\ K_{43} & K_{44} \end{bmatrix}$$

Expressing y_2, θ_2, F_2 and M_2 in the terms of y_1, θ_1, F_1 and M_1, we get

$$\begin{Bmatrix} y_2 \\ \theta_2 \\ F_2 \\ M_2 \end{Bmatrix} = \begin{bmatrix} -T_{12}^{-1}T_{11} & T_{12}^{-1} \\ T_{21} - T_{22}T_{12}^{-1}T_{11} & T_{22}T_{12}^{-1} \end{bmatrix} \begin{Bmatrix} y_1 \\ \theta_1 \\ F_1 \\ M_1 \end{Bmatrix}$$

Hence we obtain the transfer function.

$$H = \begin{bmatrix} A & B \\ C & D \end{bmatrix}$$

Where

$$A = -T_{12}^{-1}T_{11}$$

$$B = T_{12}^{-1}$$

$$C = T_{21} - T_{22}T_{12}^{-1}T_{11}$$

$$D = T_{22}T_{12}^{-1}$$

Applying the boundary conditions for fixed-free beam, we get

$$\begin{Bmatrix} y_2 \\ \theta_2 \end{Bmatrix} = B.D^{-1} \begin{Bmatrix} F_2 \\ 0 \end{Bmatrix}$$

And hence we can obtain deflection y_2 from the above equation.

4.2.1. Example

After substituting l=0.1 m, E=209e09, r0=0.005 m, t =0.002 m and NN=25, for Fig. 7, we get the following stiffness matrix-

K=

$$10^5 \times \begin{bmatrix} 7.7028 & 0.4475 & -7.7028 & 0.3228 \\ 0.4475 & 0.0322 & -0.4475 & 0.0126 \\ -7.7028 & -0.4475 & 7.7028 & -0.3228 \\ 0.3228 & 0.0126 & -0.3228 & 0.0197 \end{bmatrix}$$

Then proceeding with transfer matrix method, we get the tip deflection as tabulated in Tables 3 and 4 for different values of thickness and force, P. Results are compared with that of a solid-profiled shaft.
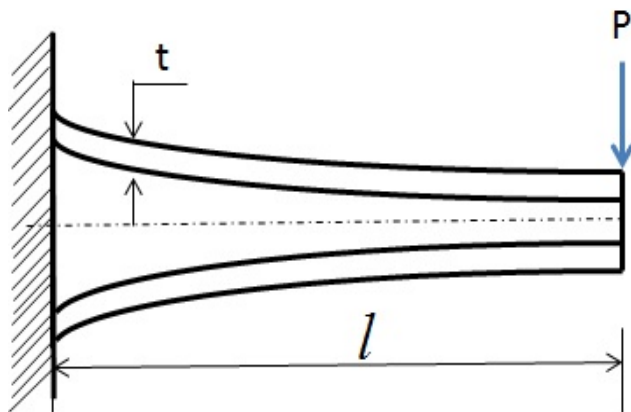

Fig. 7. Tubular Profiled Shaft with uniform thickness and vertical downward force at free end

Table 3 Deflection for varying thickness and downward force, P=1N

Thickness Value, t (m)	End Tip Deflection of Tubular Profiled Shaft (m)	End Tip Deflection of Solid Profiled Shaft (m)
0.0010	6.0327×10^{-6}	3.6365×10^{-6}
0.0015	4.7096×10^{-6}	
0.0020	4.1304×10^{-6}	
0.0025	3.8504×10^{-6}	

Table 4 Deflections for t=0.002 and varying downward force, P

Downward Force, P (N)	End Tip Deflection of Tubular Profiled Shaft (m)	End Tip Deflection of Solid Profiled Shaft (m)
1	4.1304×10^{-6}	3.6365×10^{-6}
5	2.0652×10^{-5}	1.8183×10^{-5}
25	1.0326×10^{-4}	9.0913×10^{-5}
100	4.1304×10^{-4}	3.6365×10^{-4}

Conclusion

Shaft geometry plays an important role in dynamic characteristics of rotating as well as non-rotating systems. The vibration analysis via bode plot has been done for the tubular profiled rotor system. Fig.3 shows that the amplitude increases while the critical frequency decreases as we increase the profile value of the shaft. As shown in Fig. 4, there is a large difference in frequencies even for small increase in length. Bode plot obtained in Fig. 5 shows that speeds have very little effect on the critical frequencies; however with increasing speed, the amplitude is lowered due to gyroscopic couple. Step response is also shown in Fig.6 to demonstrate the effect of gyroscopic couple with increase in speed. Combined method of TMM and FEM is demonstrated successfully for analysing non-rotating non-uniform shafts, and effect of hollowness on the deflection is shown via Tables 3 and 4.

Geared systems and other such rotary elements can be mounted instead of disks and further calculations can also be done. Simple as well as complex problems consisting of many disks (or rotary elements) and various profiled shafts can be solved via this method.

References

N. O. Myklestad, (1944), A new method for calculating natural modes of uncoupled bending vibration of airplane wings, *Journal of Aeronautical Science*, 153–162.

N. O. Myklestad, (1945), New Method of Calculating Natural Modes of Coupled Bending-Torsion Vibration of Beams, *Trans. ASME*, 61-67.

M. A. Prohl, (1945), A General Method for Calculating Critical Speeds of Flexible Rotors, *Trans. ASME*, 66, A-142-A-148.

J. W. Lund, (1974) , Stability and damped critical speeds of a flexible rotor in fluid-film bearings, *Journal of Engineering for Industry, Trans. ASME, Series B*, 96(2), 509-517.

B. T. Murphy, J. M. Vance, (1983), An improved method for calculating critical speeds and rotor dynamic stability of turbo machinery, *ASME Journal of Engineering for Power*, 105, 591-595.

R. Whalley, A. Abdul Ameer, (2009), Whirling prediction with geometrical shaft profiling, *Applied Mathematical Modeling*, 33, 3166-3177.

R.L. Ruhl, J.F. Booker, (1972), A Finite Element Model for Distributed Parameter Turborotor Systems, *Journal of Engineering for Industry*, 94(1), 126-133.

H.D. Nelson, J.M. McVaugh, (1976), The dynamics of rotor-bearing systems using finite elements, *Trans. ASME Journal of Engineering*, 98, 593–600.

Huatao Tang, Xinyue Wu, (2012), Analysis of Transfer Matrix of Non-Uniform Beam Based On Finite Element Method, *International Conference on Computer Science and Information Processing*, 242-244.

J.N. Reddy, (1984), An introduction to the finite element methods, *New York: McGraw Hill*.